Journal of Hydroscience and Hydraulic Engineering
Vol. 24, No.1 May, 2006, 1-9

INFLUENCE OF TIDAL RANGE AND RIVER DISCHARGE ON TRANSPORT OF SUSPENDED SEDIMENT IN THE OHTA FLOOD-WAY

By

Kiyosi Kawanisi

Hiroshima University, 1-4-1 Kagamiyama, Higashi-Hiroshima, Japan

Takanori Tsutsui

Mitsui Consaltant Co. Ltd, Shinjyuku-ku, Tokyo, Japan

Satoshi Nakamura

Hiroshima University, 1-4-1 Kagamiyama, Higashi-Hiroshima, Japan

and

Hitoshi Nishimaki

Ministry of Land, Infrastructure and Transport, 3-30 Hachoubori, Naka-ku, Hiroshima, Japan

SYNOPSIS

Long-duration observations of tidal currents, stratification, and suspended sediments (SS) were conducted in the Ohta flood-way to clarify the characteristics of SS transport in a tidal estuary where flow and density conditions change significantly. Deployment periods of up to 3 months allowed us to examine the effect of a flood incident and both semi-diurnal and neap/spring aspects of tides. The data revealed a semi-diurnal stratification cycle driven by tidal straining of freshwater-induced horizontal density gradient, i.e., the stratification during the ebb is stronger than that during the flood. As a result, the data of current profilers show that the velocity distribution during the ebb deviates from logarithmic law. The tidal straining and the nonlinearity of tidal wave mainly bring about the asymmetry of tidal current and bottom shear-stress. The SS transport intermittently occurs, and most of it occurs just before and after lower low water slack. Moreover, it was found out that the long term variation of SS transport is related to river discharge and to the tidal range. Peaks of the SS transport on the flood tide are higher than those on the ebb tide during the spring tide. Spatial variation of SS transport is examined from observations at three longitudinal measurement positions, which are located at about 2.8km, 5.8km and 8.8km upstream from the mouth. Additional surveys were made to examine particle size distributions of the tidal flat sediment.

INTRODUCTION

Since estuaries often lie within regions of high population and industrial activity, the effects of discharged waste on the water quality, biological productivity, and the diversity of species in estuaries have become a topic of increasing concern. The suspended sediment (SS) in estuaries play a significant role in understanding ecological and engineering problems. The flow in tidal estuaries is very complex, particularly due to tidal oscillations associated with changes in depth, mean velocity, direction of flow and density gradients affected by salt and heat. Thus, the behavior of suspended sediment in a tidal river is not similar to those in non-tidal flows and our knowledge of its behavior is insufficient. In order to acquire a better understanding of SS transport processes in tidal estuaries, long-duration measurements of velocity, density and SS concentration profiles are required so that semi-diurnal, fortnightly and seasonal timescales can be addressed. However, such measurements have been very difficult due to the unsteadiness of flow and density field. Therefore, most observations of SS in a tidal river have been limited to short durations of the tidal cycle.

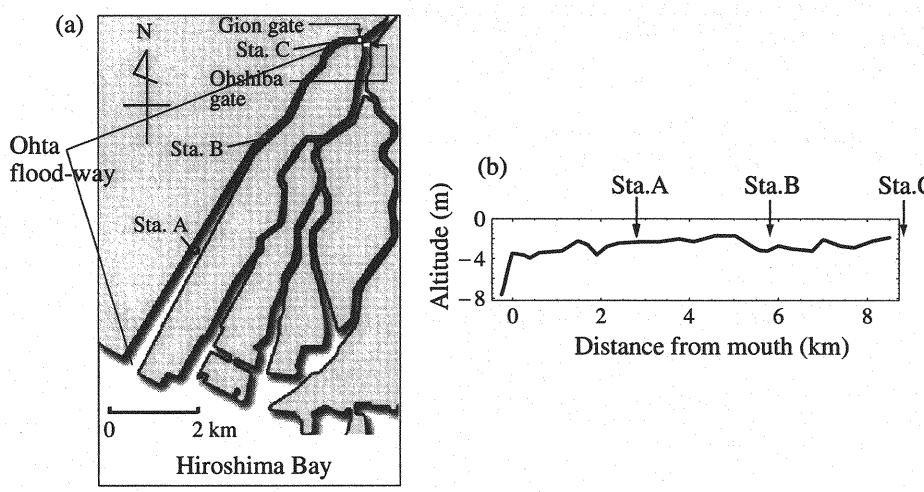

Fig. 1 (a) Study area, denoting observation points; (b) bottom topography of the Ohta flood-way

Optical and acoustical techniques can now provide extensive and detailed combined observations of current velocity and concentration of suspended particulate matter. Acoustic Doppler current profilers (aDcps) can be calibrated to provide data of the relevant quality and quantity (Holdaway et al., 1999; Kawanisi et al., 2002; Hill et al., 2003), although such calibrations could benefit from more detailed measurements of particle size (Thorne et al., 1991).

In the present study, long-duration observations of tidal current, density stratification and SS concentration were conducted in the Ohta flood-way to clarify sediment transport processes.

STUDY AREA AND OBSERVATION METHOD

As shown in Figure 1(a), the Ohta River bifurcates into some branches in the Hiroshima delta before discharging to Hiroshima Bay, and the Ohta flood-way is located on the west side of the Hiroshima delta. The Ohta estuary is tidally dominated; the tidal range of an extreme spring tide is about 4 m. The freshwater runoff from the Gion sluice, which is located at about 9 km upstream from the mouth, is usually limited to about 10 % of the Ohta River discharge. The salt water in this estuary can intrude to about 15 km upstream from the mouth. When the river discharge is greater than 400 m^3/s, the Gion sluice completely opens. As a result, the freshwater runoff from the Gion sluice is about half of the river discharge. Fig. 1(b) shows the longitudinal profile of the bottom by an echo-sounder (IDOWR Eng. Co. Ltd., 2002). The inclination of the bottom is nominal in the river channel.

Sta.A, B and C are located at points 2.8 km, 5.8 km and 8.8 km upstream from the mouth, respectively. Vertical profiles of velocity and acoustic backscatter at Sta.A and B were measured by using moored aDcps (Nortek's 1.5 MHz-NDP and 2 MHz-AqPr).

At Sta.C, a turbidimeter was located at 0.4 m above the bottom (mab). At Sta.A, salinity and temperature near the water surface (0.1 m depth) and bottom (0.4 mab) were collected to examine the density stratification in addition to the aDcp measurement. The cell size and the averaging time of NDP was configured to 0.25 m and 5 minutes, respectively. The NDP data was collected at time interval of 20 minutes. The setting of AqPr was the cell size of 0.15 m and the averaging time was 5 minutes and the time interval of acquisition was 30 minutes. The observation at Sta.A was performed for about 3 months from April 17 to July 16, 2004. The deployment period at Sta.B and C was from June 6 to July 9, 2004.

The volume scattering coefficients of aDcps, which were deduced from a sonar equation, and turbidity were calibrated with water samples.

RESULTS AND DISCUSSION

Long-term variability of stratification, velocity and SS concentration

As shown in Fig. 2(a), there were some flood incidents in the observation period. The Gion sluice completely opened on May 13 and 16, because the river discharge was greater than 400 m^3/s. The stratifi-

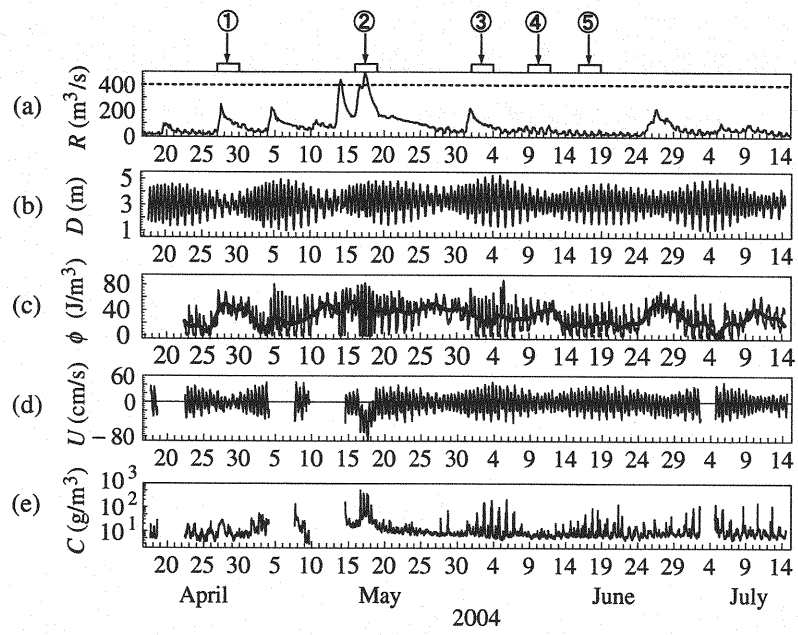

Fig. 2 Temporal variations of (a) river discharge, (b) water depth, (c) stratification parameter, (d) depth mean velocity, and (e) depth mean concentration of suspended sediment at Sta.A

cation was examined by means of the parameter ϕ proposed by (Simpson and Hunter, 1974). The parameter ϕ is the work required to bring about complete mixing and caluculated by

$$\phi = \frac{1}{D}\int_{-D}^{0} (\hat{\rho} - \rho)\, g z\, dz \qquad (1)$$

where D is the water depth, ρ water density, $\hat{\rho}$ mean density of water column, z vertical coordinate. In the present study, ϕ is estimated from densities at the surface and bottom as $gD\Delta\rho/12$, assuming the density profiles are linear because the density profile over the water column of depth D is not measured. Here $\Delta\rho$ is the density difference between the bottom and surface.

The temporal variation of stratification is shown in Fig. 2(c). It can be found that the stratification fluctuates significantly. During the spring tide, a semi-diurnal stratification cycle is higly visible. The fluctuations are driven by tidal straining of freshwater-induced horizontal density gradient (Simpson et al., 1990; Kawanisi and Tsutsui, 2004). In addition to the short cycle of stratification, the spring-neaps mixing cycle and a variation of river discharge bring about a variation of stability with a longer period as shown by the thick line, which denotes the daily mean value. The daily mean value of ϕ decreases with the increasing tidal range. The mean ϕ for the neap tide is twice as large as that of the spring tide. On the other hand, the influence of river discharge, R, on the stratification parameter, ϕ, is not a uniform state: when R is less than $400\,\mathrm{m^3/s}$, the mean ϕ increases with increasing R; mean ϕ decreases with increasing R when R is greater than $400\,\mathrm{m^3/s}$.

Fig. 2(d) shows the temporal variation of depth mean velocity. The positive sign of the streamwise velocity denotes the upstream flow. On May 17th, the depth mean velocity is negative regardless of the tidal phase because of the large runoff. The depth mean concentration of suspended sediment (SS), which is deduced from the backscatter of NDP, is shown in Fig. 2(e). The SS concentration increases intermittently during the spring tide though the concentration is low during the neap tide. The daily mean concentration for the spring tide is twice as large as that for the neap tide. In the case of flood incident of May 17th, the SS concentration of upward of $300\,\mathrm{g/m^3}$ is found.

Short-term variability of stratification, velocity, concentration and transport rate of SS

In order to understand the influence of tidal range and river discharge, we must examine the data in five periods , which are denoted by ①–⑤ shown in Fig. 2(a). The results are shown in Figs. 3–5. The bright area of the moon are shown at the left upper part of these figures. The transport rate of SS, Q_s,

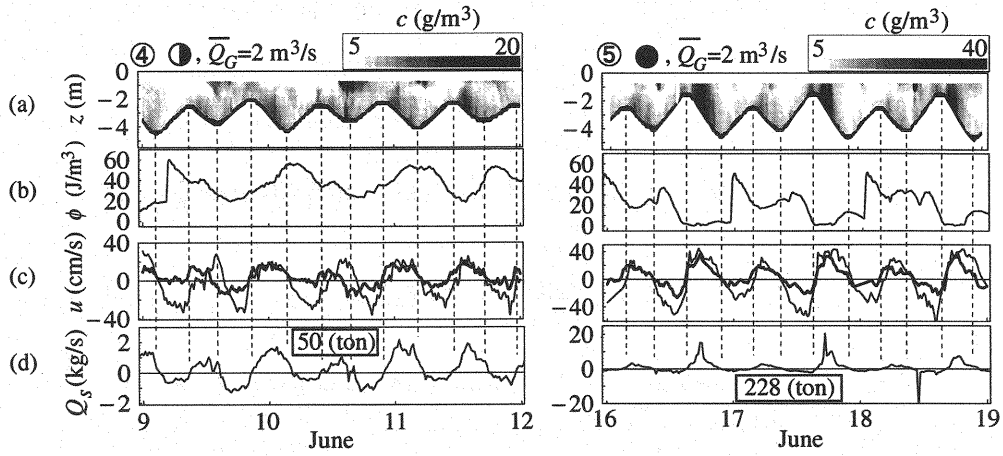

Fig. 3 Temporal variations of (a) distribution of SS concentration, (b) stratification parameter, (c) velocities at $z = -0.75$ m and $z = -0.8D$, and (d) transport rate of SS for small discharge at Sta.A; neap (left) and spring (right); number with rectangle denotes transport volume of SS for 3 days

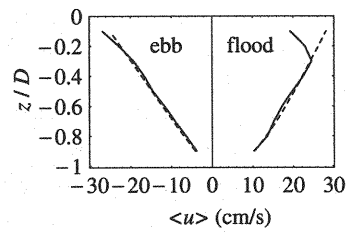

Fig. 4 Vertical profiles of phase averaged velocity; broken lines denote distributions of "log-linear" law

is estimated by

$$Q_s = B \int_{-0.9D}^{z_1} u(z)c(z)\,dz \tag{2}$$

where z_1 is the depth of first cell of NDP and that is -0.75 m in the present study. Thus, the flux of SS near the water surface and bottom is not included in Q_s because of the limitation of aDcp.

First, we examine the cases of small discharge; the results of this observation are shown in Fig. 3. The runoff from the Gion sluice, Q_G, is about $2\,\mathrm{m}^3/\mathrm{s}$. The Fig. 3④ shows the results during the neap tide. The weak tidal current took the brunt of a wind. In the area which was studied there was a land and sea breeze during the observation period. The northerly wind blew in the afternoon, so that the surface current reached a positive peak at the higher high water. Thus, the tidal straining was modulated by the wind, i.e., the wind-driven current induced by the land and sea breeze brings about diunal stratification cycle during the neap tide. The concentration of suspended sediment (SS) varied from 5 to 20 $\mathrm{g/m}^3$. The weak resuspension of sediment was found at the first half of flood tide as shown in Fig. 3④ (a)). The amount of SS transport through the cross-section during 3 days was about 50 tons.

The Fig. 3⑤ shows the results during the spring tide. Near the bottom, the flood velocity exceedes twice the ebb velocity (Fig. 3⑤ (c)). The tidal straining and the nonlinearity of tidal wave were main causes of the asymmetry of the tidal current and of bottom shear-stress (Kawanisi, 2004). Fig. 4 shows the vertical profiles of the phase averaged velocity $<u>$ for the middle of June. It is clearly found that the velocity profile is asymmetric for the ebb and flood phase. The stratification enriched with tidal straining affects the velocity profile, so that the profile in the ebb phase significantly deviates from the logarithmic law. The velocity distribution for a stratified flow is expressed by the "log–linear" law:

$$u = \frac{u_*}{\kappa}\left(\ln\frac{z+D}{z_0} + \beta\frac{z+D-z_0}{L}\right) \tag{3}$$

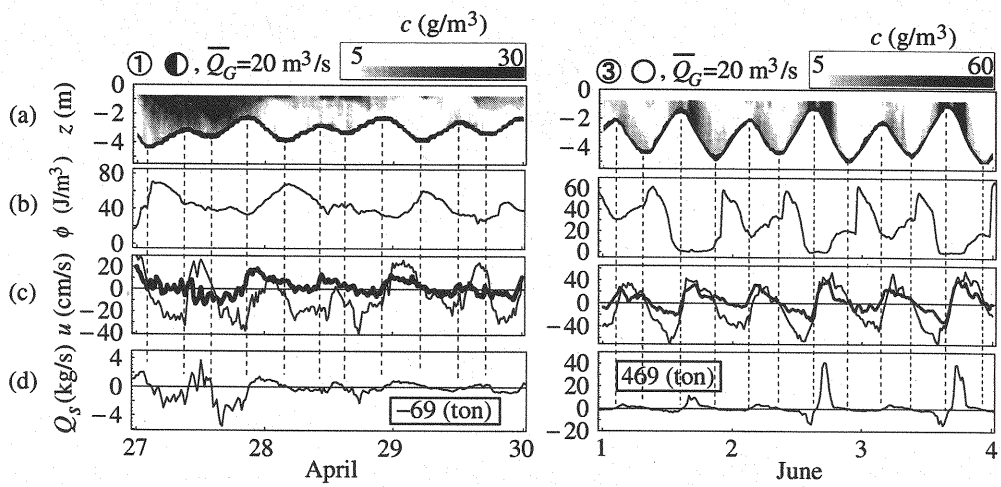

Fig. 5 Temporal variations of (a) distribution of SS concentration, (b) stratification parameter, (c) velocities at $z = -0.75$ m and $z = -0.8D$, and (d) transport rate of SS for medium discharge at Sta.A; neap (left) and spring (right); number with rectangle denotes transport volume of SS for 3 days

The distributions denoted by broken lines for the ebb and flood flow are estimated from Eq. (3) with the values ($u_* = -0.16$ cm/s, $z_0 = 5$ mm, $\beta/L = 0.2$ 1/cm) and ($u_* = 0.85$ cm/s, $z_0 = 5$ mm, $\beta/L = 0.025$ 1/cm), respectively. The friction velocity u_* for the flood phase comes up to about 5 times of u_* for the ebb phase. The above difference of β/L can explain about 70 % of the asymmetry of u_*, so that the nonlinearity of tidal wave probably brings about 30 % of the asymmetry of u_*.

The tidal velocities are distorted from sine curves, i.e., the tidal velocities take maximum values before and after the low water slack. These are characteristics of estuarine tidal flows in shallow water.

The resuspension of sediment is clearly found after the lower low water slack (LWS). Thus, the large upstream transport of SS intermittently occurs in conjunction with the resuspension. The amount of SS transport during 3 days is about 4 times as large as that for the neap tide.

In Fig. 3⑤(c), the semi-duirnal stratification cycle, which is caused by the tidal straining, is clearly evident. The mean stratification for the ebb phase is about twice as large as that for the flood phase.

Fig. 5 shows the results in the case of midium river discharge. For the neap tide ①, the velocity near the bottom is small, so that the resuspension of sediment was not found as shown in the distribution of SS concentration. The mean stratification is greater than that in the period ④. There is the same diunal stratification cycle as ④, i.e., the stratification reaches a peak just after the higher high water slack. The amount of SS transport during 3 days is negative (downstream) and is different from the small discharge case ④.

For the spring tide ③, the semi-duirnal stratification cycle is found as the small discharge case ⑤. The stratification reaches a peak just after the high water slack. The peak time leads to that in Fig. 3⑤. From Fig. 5③(a)(c), it is evident that the resuspension of sediment occures just before the lower LWS and first half of flood phase.

The velocity near the bottom for flood is greater than the velocity for ebb tide in analogy with the small discharge period. As a result, the upstream transport of SS is greater than the downstream transport. Consequently, the amount of SS transport during 3 days is positive (upstream) in contrast to the neap tide ①.

Fig. 6 shows the results in the case of flood incident. The Gion sluice was completely opened from 16:00 May 16th to 10:00 May 18th. The SS concentration become greater around the low water as shown in Fig. 6(a). The peak of SS concentration is in response to the negative peak of the velocity near the bottom. Therefore, the large downstream transport of SS takes place semi-diurnally (Fig. 6(d)). Around the high water, the downstream transport in the upper layer goes with the upstream transport in the lower layer. Since the salt water in the water column is flushed out by the large runoff, the stratification vanishes around the low water. For the phase when the salt water intrudes by flood tide, a pycnocline is formed as seen in Fig. 6(a). Therefore, the SS concentration from NDP may be overestimated because a pycnocline causes an acoustic backscatter (Seim, 1999). Fortunately, the backscatter from the pycnocline was very weak in comparison with that from SS, so that the error in the estimation of SS concentration

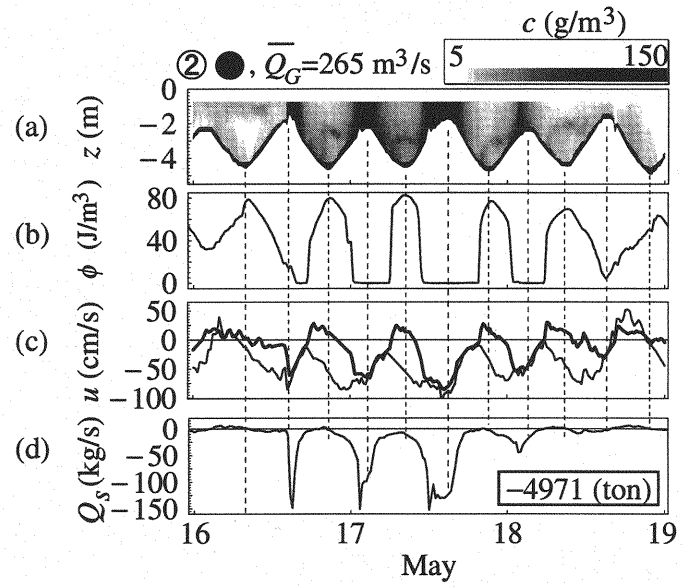

Fig. 6 Temporal variations of (a) distribution of SS concentration, (b) stratification parameter, (c) velocities at $z = -0.75$ m and $z = -0.8D$, and (d) transport rate of SS for flood incident at Sta.A; number with rectangle denotes transport volume of SS for 3 days

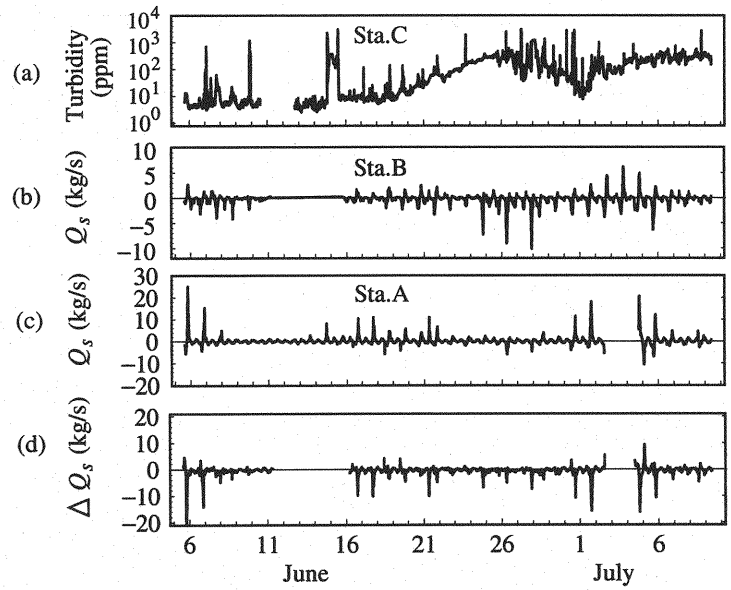

Fig. 7 Temporal variations of (a) turbidity at Sta.C, (b) transport rate of SS at Sta.B, (c) transport rate of SS at Sta.A, and (d) difference of SS transport rate between Sta.B and A

was negligible (Kawanisi et al., 2003). The amount of downstream transport during 3 days reached up to about 10 times of upstream transport in the flood tide at $\overline{Q_G} = 20\,\mathrm{m^3/s}$.

Spatial variation of SS transport rate

The temporal variations of SS transport rate at Sta.A and B are shown in Fig. 7(c) and (b), respectively. At Sta.B, which is located at a point 5.8 km upstream from the mouth, the downstream

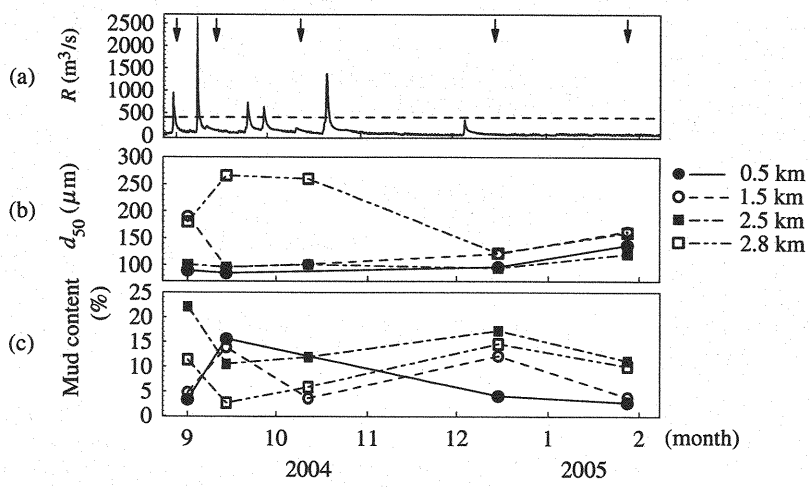

Fig. 8 Temporal variations of (a) river discharge, (b) median diameter of sediment at 4 points in tidal flat, (c) fine-grained fraction of sediment at 4 points in tidal flat

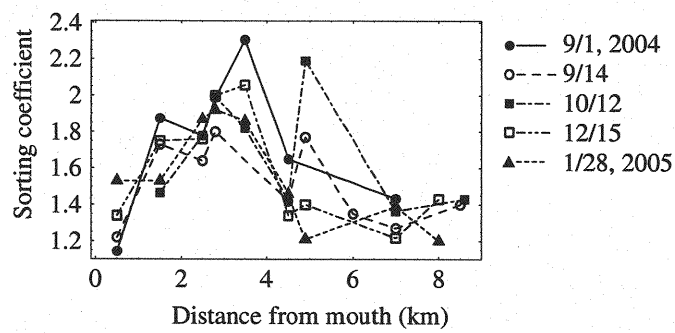

Fig. 9 Longitudinal distributions of sorting coefficient of tidal flat sediment at five points of time

transport of SS is predominant except for the period of last spring tide with the maximum tidal range. In particular, there is remarkable downstream transport from June 24th to 28th. During this period, the river discharge is large and the tidal range is small. At Sta.A on the downstream side, the positive (upstream) transport rate is remarkable. The upstream transport of SS increased with the increasing tidal range due to the nonliniarlity of tidal wave and tidal straining. The difference of transport rate between Sta.B and A, ΔQ_s = (Q_s at Sta.B) − (Q_s at Sta.A), is shown in Fig. 7(d). Since the negative value is predominant in the temporal variation of ΔQ_s, the suspended sediment is accumulated between Sta.A and Sta.B. The sedimentation rate is about 0.04 mm/day.

Fig. 7(a) shows the temporal variation of turbidity at Sta.C, which is located at a point 8.8 km upstream from the mouth and height of 0.4 mab. The turbidity was affected by the river discharge and by unknown factors rather than the tide.

Variability of tidal flat sediment

The surface sediments of the tidal flat, which are located alongside the bank, were collected at lower low waters to examine the particle size distributions. These investigations were conducted at times shown by the arrows in Fig. 8(a). On September 7th, typhoon No. 18 hit this area, so that the river discharge exceeded 2500 m^3/s. This flood incident considerably changed the surface sediment in the downstream region though the change of bottom form was small. Fig. 8(b) shows the temporal variations of median diameter at the four points. At the points near the mouth (in particular, 1.5 km upstream from the mouth), the median diameter decreased due to the flood incident. On the contrary, the median diameter increaed at 2.8 km upstream from the mouth.

The mud contents, which are defined as fraction of fine sediment ($\leq 75\,\mu$m), at the four points are shown in Fig. 8(c). Near the mouth (0.5 and 1.5 km upstream), it was clearly found that fine sediment

was deposited by the flood. At 2.5 and 2.8 km points, the mud contents decrease in a direction opposite to that near the mouth.

As mentioned previously, the direction of SS transport is usually upstream in the downstream region. This SS transport by tidal current brings the particle size distribution of the sediment back on track. It can be seen from Fig. 8(b)(c) that the sediment of tidal flat returned to its former state after about 3 months.

Fig. 9 shows longitidinal distributions of sorting coefficient of tidal flat sediment. The sorting coefficients take maximum values around 3 km upstream from the mouth. It seems that this distributions are formed by the tidal current and flood incidents, i.e., during normal times, there is an upstream net transport of fine sediments from the downstream region by the tidal current and the coarse sediments are dragged from upstream region by flood incidents. Moreover, it was found that the peak of sorting coefficient distribution moved downstream due to the flood incident on September 7th.

CONCLUSIONS

The observations of tidal current, stratification, and suspended sediment (SS) were conducted in the Ohta flood-way to clarify the characteristics of SS transport. The data were obtained using moored acoustic Doppler current profilers (aDcps). Deployment periods of upwards of 3 months enabled the influence of a flood incident and both semi-diurnal and neap/spring aspects of tide to be examined.

The density stratification varies significantly owing to the tidal straining and the river discharge. Moreover, the wind-driven current induced by the land and sea breeze causes a diunal stratification cycle during the neap tide. The tidal straining brings about the stronger stratification during the ebb. As a result, the profile of ebb current deviates from logarithmic law (Kawanisi, 2004). The effect of river discharge on the stratification did not result in a uniform state. The daily mean stratification decreases with increasing discharge when the Gion sluice is completely opened ($> 400\,\mathrm{m}^3/\mathrm{s}$).

The suspended sediment (SS) in the flood-way was intermittently tranported, i.e., the most of SS was usually transported just before and after the lower low water slack. The velocity near the bottom (bottom shear-stress) was found to be asymmetric owing to the tidal straining and the nonlinearity of tidal wave: the flood velocity is greater than ebb velocity. Consequently, the net transport of SS was upstream for the spring tide. The upstream transport increases with increasing tidal range and decreases with increasing distance from the mouth. At the flood evednt, the suspended sediment was transported downstream around the low water and the transport rate is almost zero around the high water.

A flood incident considerably changed the surface sediments of the tidal flat, which are located alongside the bank. It was clearly found that fine sediment was deposited near the mouth by the flood. The fine sediment was transported upstream by tidal current. As a result, the sediment of tidal flat returned to its former state after about 3 months.

Acknowledgement

The authours would like to thank three anonymous reviewers whose in-depth comments are appreciated.

REFERENCES

Hill, D. C., Jones, S. E. and Prandle, D. (2003). "Derivation of sediment resuspension rates from acoustic backscatter time-series in tidal waters." *Contin. Shelf Res.*, 23(1), 19–40.

Holdaway, G. P., Thorne, P. D., Flatt, D., Jones, S. E. and Prandle, D. (1999). "Comparison between adcp and transmissometer measurements of suspended sediment concentration." *Contin. Shelf Res.*, 19(1), 421–441.

IDOWR Eng. Co., Ltd. (2002). Business report for bottom sediment in the Ota and Oze River.

Kawanisi, K., Mizuno, F., Matsuyama, Y., Nagai, S. and Kotani, Y. (2002). "Sound scattering characteristics near the sea bed in northern Hiroshima bay." *Oceanography in Japan*, 11(2), 285–293.

Kawanisi, K., Tsutsui, T. and Nishimaki, H. (2003). "Dynamics of tidal flow and suspended sediments in estuary." *Ann. J. Coast. Eng., JSCE*, 48, 411–415.

Kawanisi, K. (2004). "Structure of turbulent flow in a shallow tidal estuary." *J. Hydraul. Eng., ASCE*, 131(4), 360–370.

Kawanisi, K. and Tsutsui, T. (2004). "Variability of stratification in shallow tidal estuary." *Ann. J. Hydraul. Eng.*, 48, 781–786.

Seim, H. E. (1999). "Acoustic backscatter from salinity microstructure." *American Meteorological Society*, 116, 1491–1498.

Simpson, J. H. and Hunter, J. R. (1974). "Fronts in the Irish Sea." *Narure*, 250, 404–406.
Simpson, J. H., Brown, J., Matthews, J. and Allen, G. (1990). "Tidal straining, density currents, and stirring in the control of estuarine stratification." *Estuaries*, 13(2), 125–132.
Thorne, P. D., Vincent, C. E., Hardcastle, P. J., Rehman, S. and Pearson, N. (1991). "Measuring suspended sediment concentrations using acoustic backscatter devices." *Mar. Geol.*, 98(1), 7–16.

APPENDIX – NOTATION

The following symbols are used in this paper:

B = river width;
C = depth mean concentration of suspended sediment;
c = concentration of suspended sediment;
D = water depth;
d_{50} = median diameter of sediment;
g = gravitational acceleration;
Q_G = discharge through the Gion sluice;
Q_s = transport rate of suspended sediment;
R = river discharge;
U = depth mean longitudinal velocity;
u = longitudinal velocity;
$<u>$ = averaged longitudinal velocity for ebb and flood phase;
z = vertical coordinate (origin is located water surface and upward);
z_1 = depth of first cell of aDcp;
ϕ = stratification parameter;
ρ = density of water;
$\hat{\rho}$ = depth mean density of water;
$\overline{\ }$ = daily mean.

(Received August 12, 2005 ; revised February 2, 2006)